

Axisymmetric Plasma Equilibria with Flow: a New Solver

A.J.C. Beliën, J.P. Goedbloed, and B. van der Holst

*FOM-Institute for Plasma Physics 'Rijnhuizen', Association Euratom-FOM, TEC,
P.O. Box 1207, 3430 BE Nieuwegein, The Netherlands*

Introduction

Until recently, the vast majority of investigations of waves and instabilities in astrophysical and laboratory plasmas have been carried out for static plasma configurations. Particle exhaust and extensive use of neutral beam heating in present day fusion devices cause flows that can easily reach a considerable fraction of the Alfvén speed. Such flows will definitely alter the spectrum of waves and instabilities. Therefore, a theoretical description of such systems is needed. For astrophysical plasmas this is important as well, since they always exhibit flows.

In astrophysical plasmas, the flows are often transsonic and much of the recent analytical work on the subject has focussed on such flows. The focus of this paper, however, is the numerical construction of highly accurate solutions of the stationary axisymmetric MHD equations for fusion (tokamak) as well as astrophysical plasmas (e.g., coronal loops, stellar breezes) that, in first instance, do not cross any of the sonic points, i.e., which are confined to elliptic flow regimes. The high accuracy is needed to compute without pollution the spectrum of waves and instabilities with our spectral flow solvers, see, e.g., Ref. [1].

Until now, numerical solvers for axisymmetric plasmas with poloidal and toroidal flow have been rare. Zelazny et al. [2] used an inverse coordinate approach combined with Fourier decomposition of the poloidal dependence. Since the governing differential equation is highly nonlinear in case of inverse coordinates, high accuracy is only obtained for very high resolutions. Convergence can be slow due to the high nonlinearity as well. Recent progress in the understanding of the solutions of the Bernoulli equation in terms of the least number of free parameters [3,4] and a variational description of the whole problem, has inspired us to tackle the numerical solution by solving for the flux and poloidal Alfvén Mach number and do the inversion afterwards.

In this paper we briefly describe our numerical method and solver and present first results obtained.

The Core Problem

Stationary, axisymmetric MHD equilibria are described, in a cylindrical coordinate system (R, Z, ϕ) , by a nonlinear partial differential equation for the poloidal magnetic flux function $\psi(R, Z)$

$$\nabla \cdot \left(\frac{1 - M^2}{\mu_0 R^2} \right) \nabla \psi + \frac{\partial W}{\partial \psi} = 0, \quad (1)$$

and an algebraic equation for the squared poloidal Alfvén Mach number $M^2 = M^2(R, Z) \equiv \mu_0 \rho v_p^2 / B_p^2$

$$\frac{|\nabla \psi|^2}{2\mu_0 R^2} + \frac{\partial W}{\partial M^2} = 0. \quad (2)$$

This very compact form of the set of equations is due to Goedbloed and Lifschitz [3,4] and is closely related to the underlying variational principle, W being the potential part of the Lagrangian density. The function W contains all the information of the stationary state that can be specified freely. Its definition,

$$W = W(\psi, M^2; R^2, Z^2) \equiv \frac{\Pi_1(\psi; R, Z)}{M^2} - \frac{\Pi_2(\psi)}{\gamma M^{2\gamma}} + \frac{\Pi_3(\psi; R)}{1 - M^2}. \quad (3)$$

is given in terms of three generic functions Π_i

$$\Pi_1 = \Pi_1(\psi(R, Z); R, Z) \equiv \Lambda_1(\psi) + R^2 \Lambda_3(\psi) + \Lambda_5(\psi) \Phi_{\text{grav}}(R, Z), \quad (4)$$

$$\Pi_2 = \Pi_2(\psi(R, Z)) \equiv \Lambda_2(\psi), \quad (5)$$

$$\Pi_3 = \Pi_3(\psi(R, Z); R) \equiv R^2 \Lambda_3(\psi) \left(1 - \frac{\Lambda_4(\psi)}{R^2}\right)^2. \quad (6)$$

which depend on five free flux functions, $\Lambda_i(\psi)$, and the explicit coordinates R and Z . The function Φ_{grav} is the spatial dependence of the potential of a gravitational point source. The relations between the Λ_i 's and the more physical flux functions, χ (stream function), S (entropy), H (Bernoulli function), I (toroidal momentum flux), and Ω (normal electric field) are given by:

$$\Lambda_1 \equiv \mu_0 \chi'^2 H, \quad \Lambda_2 \equiv \frac{\gamma}{\gamma - 1} \chi'^{2\gamma} S, \quad \Lambda_3 \equiv \frac{1}{2} \mu_0 \chi'^2 \Omega^2, \quad (7)$$

$$\Lambda_4 \equiv -\frac{I}{\chi' \Omega}, \quad \Lambda_5 \equiv \mu_0 \chi'^2 G M_{\text{grav}}. \quad (8)$$

A prime indicates derivation.

Details on the Numerical Solver

After the geometry, boundary conditions, and free flux functions have been specified, the algorithm used to solve Eqs. (1)–(2) is based on Picard iteration. Starting from an initial guess for ψ , the Bernoulli equation is solved for M^2 . Both ψ and M^2 are then substituted in $\partial W / \partial \psi$, while M^2 is also substituted in the differential operator part. As a consequence, the differential operator is guaranteed to be elliptic and the equation has become linear in the flux ψ . When the Picard iteration has converged, M^2 is updated and the Picard iteration is repeated until some convergence criterion on both ψ and M^2 is met.

The linearized differential equation for the flux ψ that appears in the Picard iteration scheme is discretized and solved using isoparametric bi-cubic Hermite elements similar to the approach taken for our static equilibrium solvers [5,6].

To solve the Bernoulli equation we rewrite it in the most compact form possible:

$$\tilde{\Phi} = \frac{1}{M^4} - \frac{P}{M^{2(\gamma+1)}} - \frac{Q}{(1 - M^2)^2}, \quad (9)$$

where $P \equiv \frac{\Pi_2}{\Pi_1}$, $Q \equiv \frac{\Pi_3}{\Pi_1}$, and $\tilde{\Phi} \equiv \frac{|\nabla \psi|^2}{2\mu_0 R^2 \Pi_1}$. For the slow flow domain that we are interested in, solutions are only possible if $P \leq P^\dagger(Q) \leq 1$, and $\tilde{\Phi} \leq \tilde{\Phi}^\dagger(P)$. See, Refs. [3,4] for details on the functions P^\dagger and $\tilde{\Phi}^\dagger$. The totality of solutions of the Bernoulli equation can be represented as a function of three variables, viz., $M^2 = M^2(P, Q, \tilde{\Phi})$. Using a well established root-finding

algorithm to solve the Bernoulli equation (9) is a computationally intensive task. The above description indicates the possibility to calculate M^2 *a priori* on a grid of P , Q , and $\tilde{\Phi}$ values to exploit interpolation of the tabulated values to obtain M^2 on the grid points. As an option in our code, we have implemented a tri-linear database interpolation scheme to solve the Bernoulli equation. We have tested its performance with respect to the direct root-finding option.

In table 1, the CPU time needed to compute an equilibrium for a torus geometry with circular cross-section and with a gravitational point source are listed for both the use of database interpolation and direct root-finding. It is clear from this table that the interpolation is approximately 20% to 25% faster than direct root-finding. The overhead of reading in the Bernoulli database is only visible for the lowest grid resolutions. While database interpolation is faster,

$N_r \times N_p$	10×10	20×20	40×40	80×80
$N_P \times N_Q \times N_{\tilde{\Phi}}$				
$100 \times 100 \times 100$	3.6	9.8	38.9	192.3
$400 \times 100 \times 100$	3.6	9.8	38.9	192.2
$800 \times 100 \times 100$	3.7	9.9	39.1	193.0
$\infty \times \infty \times \infty$	3.6	12.8	53.6	252.4

Table 1: Single C98 CPU-time in seconds needed to calculate a typical solution for different grid (horizontal) and Bernoulli database (vertical) resolutions. The bounds of the Bernoulli database are: $0 \leq P \leq 1$, $0 \leq Q \leq 10^4$, $0 \leq \tilde{\Phi} \leq 10^3$. The last horizontal line represents the direct root-finding method.

it is always less accurate than direct root-finding as shown by the value of the eigenvalue A in table 2. The eigenvalue A is related to the amplitude of W . Its value is fixed by the conditions imposed on ψ on the magnetic axis. Other disadvantages of the database method are higher

$N_r \times N_p$	10×10	20×20	40×40	80×80
$N_P \times N_Q \times N_{\tilde{\Phi}}$				
$100 \times 100 \times 100$	0.057088346	0.057086047	0.057085935	0.057085929
$400 \times 100 \times 100$	0.058994803	0.058992427	0.058992307	0.058992300
$800 \times 100 \times 100$	0.059051928	0.059049559	0.059049443	0.059049437
$\infty \times \infty \times \infty$	0.059070707	0.059068328	0.059068213	0.059068206

Table 2: The eigenvalue A for a typical solution for different grid (horizontal) and Bernoulli database (vertical) resolutions. The last horizontal line represents the direct root-finding method.

memory consumption and the fixed bounds of the database variables. If one changes the amplitudes of the free flux functions one might end up outside the domain covered by the database and a new one has to be computed first. If the focus is on accuracy and CPU consumption does not impose limitations, then root-finding is preferable.

First Results

The implementation of the numerical algorithm in our code works. High accuracy can be obtained for a modest resolution due to the h^4 convergence behavior of the exploited bi-cubic Hermite elements. For example, the eigenvalue A shown in table 2, that is obtained with direct root-finding and a grid resolution of 80×80 , is converged up to the second to last digit

shown. Currently, our code can handle three types of geometries: torus geometry for tokamak applications, cylinder geometry for coronal loop applications, and spherical geometry for stellar breeze applications. In Fig. 1 we show first results obtained for a flowing plasma in a torus with a strong gravitational point source at the torus origin, and a stellar breeze solution for a rotating star with a dipole magnetic field structure.

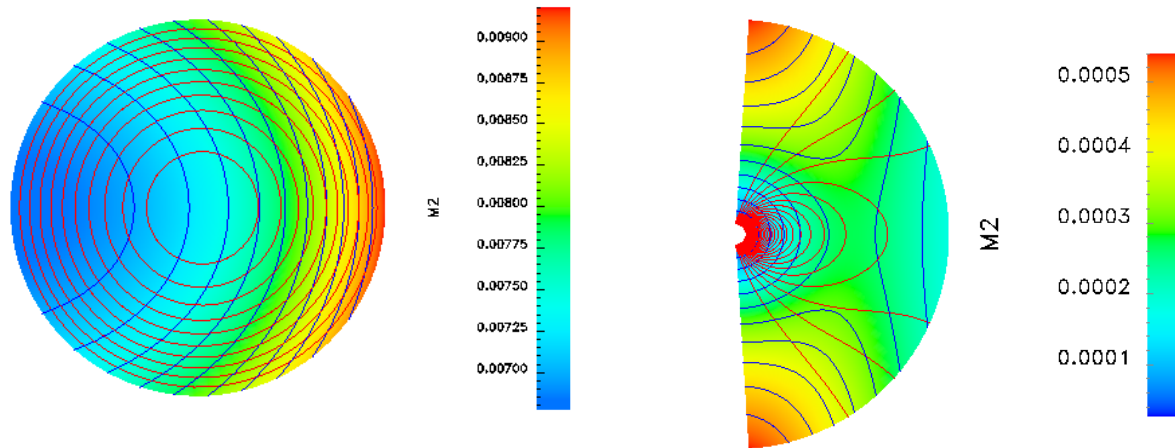


Figure 1: *Contour lines for the flux (red) and squared poloidal Alfvén Mach number (blue) in poloidal cross-sections: (left) A flowing plasma in a torus geometry with a strong gravitational point source at the origin on the symmetry axis. The aspect ratio is 10 and the symmetry axis is on the left. (right) A stellar breeze solution. Twenty stellar radii are plotted and only the part on the right of the symmetry axis is shown.*

Outlook

Since we have shown that the implementation of our numerical algorithm results in accurate stationary axisymmetric plasma equilibria which are confined to elliptic flow regions, we can confidentially investigate the properties of such equilibria and study the spectrum of waves and instabilities with our new set of spectral codes.

References

- 1 B. van der Holst, A.J.C. Beliën, and J.P. Goedbloed, *Phys. Rev. Lett.* **86**, 2865 (2000).
- 2 R. Zelazny, R. Stankiewicz, A. Galkowski, S. Potemski, and R. Pietak, *JET Report JET-R(91)05*, 1991.
- 3 J.P. Goedbloed and A. Lifschitz, *Phys. Plasmas* **4**, 3544 (1997).
- 4 J.P. Goedbloed and A. Lifschitz, to appear (2000).
- 5 G.T.A. Huysmans, J.P. Goedbloed, and W. Kerner, *Phys. Fluid* **B5**, 1545 (1993).
- 6 A.J.C. Beliën, S. Poedts, and J.P. Goedbloed, *Comp. Phys. Comm.* **106**, 21 (1997).